Zinc Ions Induce the Unfolding and Self-Association of Boar Spermadhesin PSP-I, a Protein with a Single CUB Domain Architecture, and Promote Its Binding to Heparin†

María A. Campanero-Rhodes,‡ Margarita Menéndez,‡ José L. Sáiz,‡ Libia Sanz,§ Juan J. Calvete,§ and Dolores Solís*,‡

Instituto de Química Física Rocasolano, CSIC, Serrano 119, 28006 Madrid, Spain, and Instituto de Biomedicina de Valencia, CSIC, Jaume Roig 11, 46010 Valencia, Spain

Received December 23, 2005; Revised Manuscript Received May 12, 2006

ABSTRACT: Spermadhesins are a family of seminal plasma proteins composed of a single CUB domain, which appear to be involved in various aspects of the fertilization process in pigs. PSP-I and PSP-II, the most abundant porcine spermadhesins, occur in seminal plasma as noncovalent heterodimers devoid of heparin-binding capability. Of note is the stability of this dimer, which is significantly affected by physiologically relevant conditions such as Zn^{2+} ions. Here, we show that PSP-I and PSP-II when separated appear to conserve the overall fold of the CUB domain observed in the crystal structure of the PSP-I/PSP-II heterodimer, as concluded from gel filtration, analytical ultracentrifugation, differential scanning calorimetry, and circular dichroism analyses. However, Zn^{2+} concentrations in the range of those found in boar seminal plasma induce the unfolding and self-association of PSP-I, apparently as a consequence of the exposure of hydrophobic core residues, whereas they have no effect on PSP-II. Remarkably, Zn^{2+}-denatured and self-associated (but not structured monomeric) PSP-I is retained on a heparin column, resembling the behavior of free PSP-I and homologous spermadhesins of the heparin-binding fraction of boar seminal plasma, which also exhibit different aggregation states. Thus, the modulation of the structural organization and heparin-binding ability of PSP-I by Zn^{2+} might be a physiological phenomenon in seminal plasma.

The interaction of heparin and heparan sulfate with heparin-binding proteins plays important roles in numerous physiological and pathological processes. Heparin binds a large variety of proteins, including enzymes and enzyme inhibitors, growth factors and their receptors, chemokines, lipid- and membrane-binding proteins, cell adhesion proteins, and microbial receptors. The seminal plasma from many mammalian species also contains heparin-binding proteins that bind to the sperm surface at ejaculation and appear to mediate sperm capacitation induced by glycosaminoglycans present in the female reproductive tract (*1*). In the boar, the major heparin-binding proteins belong to the spermadhesin family.

Spermadhesins are 12−16 kDa proteins consisting of a single CUB domain, which have been found in the seminal plasma and/or attached to the spermatozoal surface of a variety of mammalian ungulate species (e.g., boar, bull, stallion, and ram) (*2*, *3*). Besides their heparin-binding ability, members of this family have also been shown to exhibit binding-activity for zona pellucida glycoproteins, serine protease inhibitors, and/or phospholipids (*4*−*6*), suggesting that they may be involved in different steps of the complex fertilization process. In the boar, spermadhesins represent more than 80% of the total protein content of seminal plasma; their concentration ranges from 0.6 to 7 mg mL^{-1} (*7*). PSP-I and PSP-II, the most abundant porcine spermadhesins, occur as noncovalent heterodimers. The isolated PSP-II subunit exhibits mannose-6-phosphate and heparin binding abilities (*8*), whereas conflicting results concerning the heparin-binding ability of PSP-I have been reported (*9*−*11*). These binding sites are nonetheless cryptic in the heterodimer, which is typically isolated from the nonheparin-binding fraction of boar seminal plasma (*9*). The other porcine spermadhesins, AWN-1, AQN-1, AQN-3, and excess free PSP-I, constitute the heparin-binding fraction of seminal plasma and occur in different aggregation states (*12*, *13*), which are predicted to be of functional significance. For example, only nonaggregated AWN-1 and AQN-3 are able to interact with phospholipid matrixes (*12*), suggesting that this spermadhesin subpopulation can bind directly to sperm membrane lipids. Aggregated spermadhesins could then become coated on top of this first layer, serving as stabilizing factors that protect the acrosome membrane from premature acrosome reactions. This spermadhesin coating would subsequently be released during sperm capacitation.

The crystal structure of the PSP-I/PSP-II heterodimer was solved at 2.4 Å resolution (*14*), revealing the architecture of the CUB domain. Each subunit consists of a compact ellipsoidal beta-sandwich organized into two five-stranded

† This work was supported by DGICYT (BQU2000-1501-C02-02, BQU2003-03550-C03-03, BIO2003-01952, and BFU2004-1432).

* To whom correspondence should be addressed. E-mail: d.solis@iqfr.csic.es.

‡ Instituto de Química Física Rocasolano.

§ Instituto de Biomedicina de Valencia.

10.1021/bi052621g CCC: $33.50
Published on Web 06/15/2006

(parallel and antiparallel) beta sheets, whereas the hydrophobic residues that define the CUB signature (*15*) are tightly packed within the protein core. However, no information on the architecture and stability of isolated PSP-I and PSP-II and on the structural organization of spermadhesins from the heparin-binding fraction is available. Furthermore, the nature of the self-association of spermadhesins is unknown. It is clear that seminal plasma is a complex solvent environment, and therefore, the interactions of spermadhesins with other molecules and/or cosolute effects may govern protein behavior. Indeed, we have recently observed (*16*) that in the presence of physiological concentrations of Zn^{2+}, a cation unusually abundant in boar seminal plasma (0.3−0.7 mM) (*17*, *18*), the thermostability of the PSP-I/PSP-II heterodimer decreases significantly, and the dissociation of the heterodimer, occurring at low nanomolar protein concentrations, is promoted. Although the integrity of the heterodimer in seminal plasma seems to be guaranteed by the high concentration of PSP-I/PSP-II, cryptic binding sites in the heterodimer subunits could be exposed upon dilution of the protein in the female genital tract.

In this work, we have examined the structural organization of separate PSP-I and PSP-II and the effect of Zn^{2+} on such organization. Information on the quaternary state and hydrodynamic behavior of the proteins was obtained by FPLC gel filtration and analytical ultracentrifugation, whereas their thermal stability and conformation were evaluated using differential scanning calorimetry and circular dichroism. The results reveal a dramatic effect of zinc on the stability and heparin-binding ability of PSP-I and provide a rationale for the simultaneous occurrence in seminal plasma of PSP-I forms with different conformational states and ligand-binding capabilities.

EXPERIMENTAL PROCEDURES

Isolation of Spermadhesins PSP-I and PSP-II from the PSP-I/PSP-II Heterodimer. The PSP-I/PSP-II heterodimer was isolated from the nonheparin-binding fraction of the seminal plasma of German Landrace boars by size-exclusion chromatography on Sephadex G-50, and the PSP-I and PSP-II subunits were separated by reverse-phase HPLC on a C18 column using a linear gradient of 0.1% trifluoroacetic acid in water (solution A) and 0.1% trifluoroacetic acid in acetonitrile (solution B) (*9*).

Gel Filtration Chromatography. Gel filtration was carried out at 20 °C in a Superose 12 HR 10/30 column (Pharmacia Biotech) equilibrated with 10 mM Tris/HCl at pH 7.8, 0.15 M NaCl (TBS[1]) containing 0.02% NaN_3, and, where stated, $ZnCl_2$ or $CaCl_2$ at the indicated concentration. The flow rate was 0.5 mL min^{-1}, and the elution was monitored at 280 nm. Control proteins were chromatographed under similar conditions.

Analytical Ultracentrifugation. Sedimentation equilibrium experiments were performed by centrifugation of 80-μL samples of 0.3−0.6 mg mL^{-1}concentration at 30 000*g* and 20 °C in an Optima XL-A analytical ultracentrifuge (Beckman Instruments, Inc.) equipped with UV−Vis optics and an An50Ti analytical rotor, using 12 mm path length double-sector six-channel centerpieces with quartz windows. Data were collected at 0.003 cm radial step size with five replicates. Under these conditions, hydrodynamic equilibrium was reached before 12 h of centrifugation because the same results were obtained from scans taken at 12 and 14 h. Baseline offsets were determined from radial scans of the samples run for 6 h at 160 000*g*. Weight-average molecular masses, M_w, were calculated with the XLAEQ program using the signal conservation algorithm (*19*).

Sedimentation velocity experiments were carried out in the same ultracentrifuge at 150 000*g* and 20 °C, using 400-μL samples of 0.45 mg mL^{-1} concentration. Up to 20 scans were carried out every 5 min, also at 0.003 cm radial step size, and the corresponding buffer signal was subtracted. Sedimentation coefficients were calculated using the programs XLAVEL, supplied by Beckman, and SEDFIT (*20*) with similar results.

The partial specific volume and degree of hydration of PSP-I were calculated from the amino acid (Swiss-Prot AC: P35495) and carbohydrate (*21*) composition to be 0.716 cm^3 g^{-1} and 0.413 g_{water} $g_{protein}^{-1}$, respectively, using the Sednterp software (*22*). An average carbohydrate composition of 3 mannoses, 1 galactose, 1 fucose, 1 *N*-acetyl-neuraminic acid, and 5 *N*-acetyl-hexosamine residues, which yields a calculated molecular mass of 14 095 Da, very close to the average mass experimentally determined by mass spectrometry (14 089 Da), was used for the calculation. Solvent densities at 20 °C were calculated using the data set included in the Sednterp program plus the density increments for $ZnCl_2$ experimentally determined using a Paar Precision Density Meter DMA 02D. Solvent viscosity was also calculated using the Sednterp program.

The PSP-I samples were extensively dialyzed at 4 °C against TBS alone or with 2 mM EDTA. The samples containing either $ZnCl_2$ or $MgCl_2$ were prepared by the addition of the corresponding salt to the PSP-I solution in TBS and to the reference buffer followed by preincubation for 12 h at 4 °C before ultracentrifugation, unless otherwise indicated.

Differential Scanning Calorimetry. For DSC, the samples were dialyzed extensively against a 20 mM Hepes buffer at pH 7.0, in the absence or presence of $ZnCl_2$. The DSC measurements were performed using a Microcal MCS instrument at a heating rate of 0.33 °C min^{-1} under an extra constant pressure of 2 atm. The standard Microcal Origin software was used for data acquisition and analysis. The excess heat capacity functions were obtained after the subtraction of the buffer baseline. The reversibility of the transitions was checked by performing a second scan after the first run.

Circular Dichroism Spectra. CD spectra were acquired for PSP-I solutions in 20 mM Hepes buffer at pH 7.0 in a JASCO J-720 spectropolarimeter fitted with a water-bath thermostated cell holder or in a J-810 spectropolarimeter equipped with a Peltier temperature control system, using a bandwidth of 0.2 nm and a response time of 2 s. Far-UV spectra were recorded in 0.02 and 0.1 cm path length quartz cells at a protein concentration of 1 and 0.2 mg mL^{-1}, respectively. Near-UV spectra were registered at 1.0 mg mL^{-1} protein concentration in 1 cm path length cells. For all CD spectra, the corresponding buffer baseline was subtracted. The observed ellipticities were converted to mean

[1] Abbreviations: CD, circular dichroism; DSC, differential scanning calorimetry; TBS, Tris buffered saline.

residue ellipticities using mean molecular masses per residue of 129.26, 125.65, and 127.4 for PSP-I, PSP-II, and PSP-I/PSP-II heterodimer, respectively. These values were calculated by dividing the average molecular masses obtained by MALDI mass spectrometry (14 089 Da, 14 575 Da, and 28 664 Da for PSP-I, PSP-II, and PSP-I/PSP-II, respectively) by the number of amino acid residues of the mature protein (109, 116, and 225). Secondary structure elements were calculated from the CD spectra using the Lincomb method (*23*) as previously described (*24*).

Thermal denaturation experiments were carried out by increasing the temperature from 5 to 70 °C at a scanning rate of 0.33 °C min^{-1}, allowing the temperature to equilibrate for 5 min before recording the spectrum. Variations in ellipticity were monitored every 0.2 °C at one or more wavelengths and the complete spectrum was recorded every 5−15 °C, after equilibration for 1−5 min at the selected temperature. No significant differences between the ellipticity values registered at a given wavelength and those obtained from the spectrum were observed. Thermal denaturation profiles were described in terms of the following sigmoidal function:

$$\Theta(T) = \Theta_D(T) - [\Theta_D(T) - \Theta_N(T)]/\{1 + \exp[A(T - T_{1/2})/RTT_{1/2}]\}$$

where T is the absolute temperature, $T_{1/2}$ is the half-transition temperature, R is the gas constant, A is the temperature constant accounting for the ratio between the native and denatured states, and Θ_D (T) and Θ_N (T) are the ellipticities of the denatured and native states at temperature T (*16*). Θ_D and Θ_N were approximated as linear functions of temperature: $(\Theta_i(T) = \Theta_i(T_0) + m_i(T - T_0)$, where T_0 is a reference temperature, and m_i is the temperature dependence of Θ_i for i = N or D).

Affinity Chromatography on Heparin-Acrylic Beads. A sample of PSP-I in TBS containing either 2 mM EDTA or 1 mM $ZnCl_2$ was applied to a 5-mL heparin acrylic bead column (Sigma) equilibrated with the same buffer. The bound protein was eluted by the addition of 1 M NaCl to the buffer. The flow rate was 15 mL h^{-1}, and the elution was monitored at 280 nm.

RESULTS

Gel Filtration Studies. On gel filtration chromatography, PSP-I eluted predominantly as a single sharp peak (Figure 1A) with an apparent molecular mass of about 14 kDa (elution time 28.4 min), as previously reported (*8*). PSP-II also eluted as a monomer, although a variable percentage depending on the batch of aggregated material was also observed (data not shown). The elution time of PSP-I/PSP-II was 26 min, consistent with the time predicted for the dimer. When an equimolar mixture of PSP-I and PSP-II was chromatographed, a single peak at 26 min was obtained (Figure 1A), highlighting the ability of the two proteins to reassociate into heterodimers.

The addition of increasing concentrations of $ZnCl_2$ resulted in a progressive broadening of the elution peak for PSP-I, with a displacement of the maximum toward shorter elution times and the concomitant appearance of earlier-eluting species (Figure 1B). Thus, in the presence of 2 mM Zn^{2+},

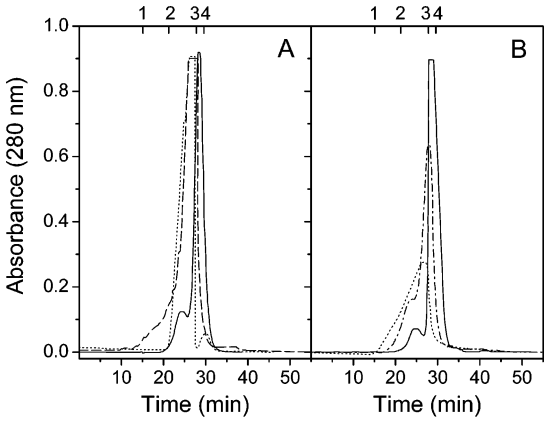

FIGURE 1: Gel filtration chromatographic behavior of PSP-I. The effect of Zn^{2+}. (A) PSP-I alone (—) or in the presence of an equimolar amount of PSP-II (----) was chromatographed on a Superose 12 column equilibrated with 10 mM Tris/HCl at pH 7.8, 0.15 M NaCl, and 0.02% NaN_3 (TBS); comparison with the PSP-I/PSP-II heterodimer (....). (B) PSP-I samples in TBS containing 3 mM EDTA (—), 0.2 mM Zn^{2+} (-·-·-), or 2 mM Zn^{2+} (....) were chromatographed on the same column equilibrated with the corresponding buffer. The elution positions of 1, Blue dextran (2000 kDa); 2, β-amylase (200 kDa); 3, chymotrypsinogen (25 kDa); and 4, cytochrome C (12.4 kDa) are indicated in the top axes.

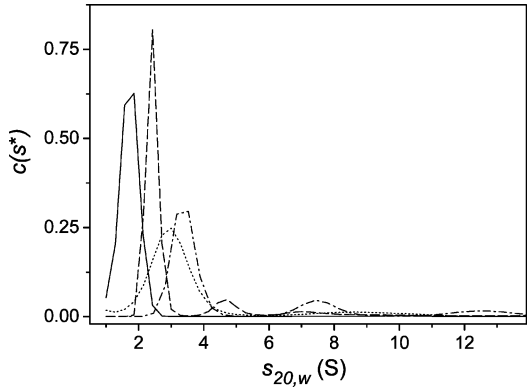

FIGURE 2: Effect of Zn^{2+} on the sedimentation coefficient distribution of PSP-I. The sedimentation velocity behavior of PSP-I in the absence (—) or presence of 0.5 mM (----), 2 mM (....), or 5 mM (-·-·-) Zn^{2+} was analyzed at 150 000g after a 48 h preincubation period at 4 °C. Experimental data were analyzed using SEDFIT.

PSP-I eluted as a manifestly asymmetric peak with a maximum at 26.6 min. This behavior was reversed by the subsequent addition of EDTA (not shown). However, the presence of 3 mM Ca^{2+} neither produced any observable alteration in the chromatographic behavior of PSP-I nor counteracted the effect of Zn^{2+}. No effect of Zn^{2+} on the chromatographic behavior of PSP-II was observed.

Analytical Ultracentrifugation Studies. The molecular mass of PSP-I and the particle hydrodynamic behavior in the presence and absence of Zn^{2+} were further investigated by analytical ultracentrifugation.

Sedimentation velocity studies of PSP-I revealed a single component (Figure 2) with an $s_{20,w}$ value of 1.8 S, consistent with an apparent molecular mass of 14.1 kDa (Table 1). The translational friction coefficient (f/f_o = 1.23) and the equivalent radius (1.59 nm) for the anhydrous sphere with the same sedimentation coefficient were estimated from the experimental data using the Sednterp program. The approximation of the anhydrous protein shape to either prolate or oblate ellipsoids of revolution with the same f/f_o value yielded

Table 1: Sedimentation Coefficient and Distribution of PSP-I Species in the Absence and Presence of Zn^{2+} [a]

	12 h preincubation period			48 h preincubation period		
$[Zn^{2+}]$ (mM)	$s_{20,w}$ (S)	$M_{w,app}$ (kDa)	RA[b] (%)	$s_{20,w}$ (S)	$M_{w,app}$ (kDa)	RA[b] (%)
0	1.80 ± 0.05	14.0 ± 0.5	99	1.8 ± 0.05	14 ± 0.5	99
0.5	1.80 ± 0.05	15.0 ± 0.5	90	2.5 ± 0.05	20.0 ± 0.6	89.5
	4.0 ± 0.1	45.0 ± 1.5	9	4.7 ± 0.1	56 ± 2	8.5
				7.0 ± 0.1	112 ± 2	2
2	2.50 ± 0.05	20.0 ± 0.6	86	3.05 ± 0.05	29.0 ± 0.7	94
	4.8 ± 0.1	59 ± 1.5	14	6.5−12[c]	90−250	6
5	2.90 ± 0.05	27.0 ± 0.7	87	3.40 ± 0.05	37.0 ± 0.8	75
	5.2 ± 0.1	65 ± 2	13	7.5 ± 0.1	120 ± 2	16
				12.4 ± 0.15	270 ± 5	9

[a] The samples were prepared by the addition of $ZnCl_2$, at the indicated concentration, to a PSP-I solution (0.45 mg mL^{-1}) in TBS and subsequently incubated for either 12 or 48 h at 4 °C before running the sedimentation velocity experiments. [b] RA, relative abundance; the estimated error is 1%. [c] The species sedimenting in a broad distribution within these $s_{20,w}$ values.

particles with axial *a*/*b* ratios of 2.18 and 2.23, respectively. Thus, PSP-I would be hydrodynamically equivalent to an anhydrous prolate ellipsoid with axial dimensions of 5.2 nm (2a) and 2.4 nm (2b) or to an oblate ellipsoid with axial dimensions of 4.0 nm (2a) and 1.8 nm (2b). These dimensions are satisfactorily comparable to those reported for the ellipsoidal PSP-I and PSP-II subunits in the crystal structure of the PSP-I/PSP-II heterodimer (4.2 × 2.7 × 2.3 nm^3) (*14*).

The addition of Zn^{2+} resulted in an increase in the $s_{20,w}$ value of the predominant PSP-I species and the appearance of faster-sedimenting components (Figure 2), with the sedimentation coefficient distribution *c(s)* being dependent on the concentration of Zn^{2+} and on the length of the previous incubation period (Table 1). When samples were analyzed 12 h after the addition of 0.5−2 mM Zn^{2+} to a PSP-I solution, the main component exhibited $s_{20,w}$ values ranging from 1.8 to 2.5 S, depending on the concentration of Zn^{2+}, and a small peak centered at 4.0−4.8 S, accounting for 9−14% of the protein, was also observed. The molecular mass distribution (Table 1) could be compatible with the existence of a monomer−dimer equilibrium, together with a subsequent tetramerization process proceeding at a slow rate in the time-scale of sedimentation. Longer preincubation periods (48 h) resulted in higher $s_{20,w}$ values, and the dimers became the predominant species, although small fractions of heavier components were also detected. At 5 mM $ZnCl_2$, significantly above the range of Zn^{2+} concentrations found in boar seminal plasma, the sedimentation coefficients and the molecular mass distribution could be compatible with dimers still being the predominant species, along with the slow formation of tetramers and higher-order oligomers.

The sedimentation equilibrium data for PSP-I alone showed no dependence on protein concentration (Figure 3) and could be fitted to a single ideal component with a weight-average molecular weight of 16 600 ± 600, either in the presence or absence of 2 mM EDTA. This value is 2.5 kDa higher than the molecular mass experimentally determined by mass spectrometry (14 089 Da). Although the estimation of the partial specific volume might be affected by the heterogeneous glycosylation of PSP-I (*21*), the uncertainty in its value cannot account for the observed difference in molecular mass. However, a closer inspection of the sedimentation velocity results for PSP-I unveils the presence of a minute percentage (1.4%) of high molecular mass species (up to 205 kDa), which might account for the increased average molecular weight. Because of the small proportion of these species, their nature was not investigated further.

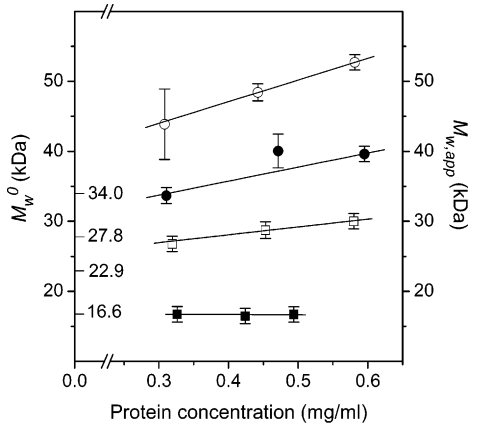

FIGURE 3: Zn^{2+}-induced dependence on protein concentration of the weight-average molecular mass of PSP-I determined by sedimentation equilibrium. PSP-I samples at different loading concentrations were analyzed at 30 000*g* in the absence (■) or presence of 0.2 mM (□), 1 mM (●), or 5 mM (○) Zn^{2+}, after a 12 h preincubation period at 4 °C. The scans were taken after 12 h of centrifugation. Apparent weight-average molecular masses are shown on the right *y*-axis and the molecular masses obtained by extrapolation to zero protein concentration are indicated on the left *y*-axis.

In the presence of Zn^{2+}, the sedimentation equilibrium profiles could not be fitted to a single component and became dependent on protein concentration (Figure 3), thus revealing self-association. The radial absorbance distribution data of PSP-I in the presence of 0.2−1 mM Zn^{2+} could be well fitted by a monomer/dimer/tetramer equilibrium. At 5 mM Zn^{2+}, somewhat higher weight-average molecular masses were obtained, in agreement with the pattern of molecular mass distributions observed in the sedimentation velocity experiments.

No increase in the molecular mass of PSP-I was observed in the presence of Mg^{2+} concentrations up to 10 mM, and the average molecular weight (16 600 Da) was independent of protein concentration (data not shown). When a PSP-I solution in 20 mM sodium acetate/acetic acid buffer at pH 6.0 was analyzed, a slightly higher weight-average molecular weight (17 800 ± 300 Da) was observed, possibly indicating some self-association, but most importantly, at this pH, the molecular mass remained invariant upon the addition of Zn^{2+} at a final concentration of 1 mM. This marked influence of the pH is suggestive of the possible involvement of histidine residues in Zn^{2+} coordination.

Differential Scanning Calorimetry. Although certain batch-to-batch variations were observed in the thermal denaturation parameters obtained for PSP-I and PSP-II, the DSC data consistently showed that the thermal stability of the isolated subunits is substantially smaller than that of the PSP-I/PSP-II heterodimer (Figure 4). Average transition temperatures of the different batches dropped from 60.7 ± 0.3 °C, as previously found for the heterodimer (*16*, *24*), to 41 ± 1 °C for isolated PSP-I and 51.6 ± 0.2 °C for PSP-II, with a large simultaneous decrease in the apparent enthalpies of denaturation (Table 2). Nevertheless, when an equimolar mixture

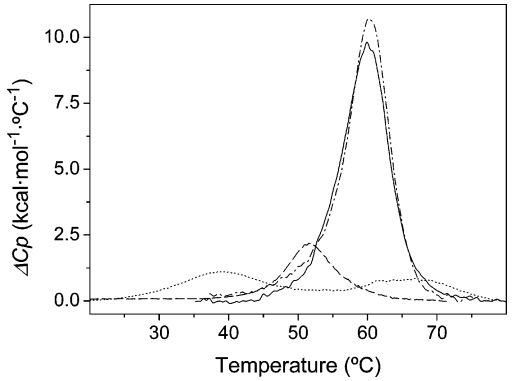

FIGURE 4: DSC profiles of the thermal denaturation of separate and pooled PSP-I and PSP-II. The excess heat capacity function (ΔC_p) of PSP-I (....), PSP-II (----), and an equimolar mixture of PSP-I and nonaggregated PSP-II (—) was determined at a scanning rate of 20 °C h^{-1} in 20 mM Hepes at pH 7. The dash−dot line (-·-·-) corresponds to the control PSP-I/PSP-II heterodimer (*14*).

Table 2: Thermal Denaturation Parameters of Spermadhesins PSP-I and PSP-II as Determined by Circular Dichroism ($T_{1/2}$) and Differential Scanning Calorimetry (T_m, ΔH_{cal})[a]

spermadhesin	$[ZnCl_2]$ (mM)	$T_{1/2}$ (°C)	T_m (°C)	ΔH_{cal} (kJ mol^{-1})
PSP-I		43.6 ± 0.6	41 ± 1	77 ± 10
	1	27.3 ± 0.4	n.d.	n.d.
	4	24.3 ± 0.5	27.7 ± 0.5	n.d.
PSP-II		52.6 ± 0.6	51.6 ± 0.2	87 ± 5
	4	50.0 ± 0.4	51.1 ± 0.2[b]	73 ± 6
PSP-I + PSP-II[c]		n.d.	60.1 ± 0.1	390 ± 10
PSP-I/PSP-II[d]		62.2 ± 0.5	60.7 ± 0.3	405 ± 17
	4	46.8 ± 0.2	51.8 ± 0.3	240 ± 10

[a] Data reported previously for the PSP-I/PSP-II heterodimer are also included for comparative purposes. [b] Data obtained at 5 mM Zn^{2+}. [c] Using a PSP-II preparation containing <5% of aggregated material. [d] Data from ref 14; n.d., not determined.

of PSP-I and PSP-II was analyzed, the corresponding heat-capacity curve approached that of the heterodimer, with the degree of recovery being PSP-II batch-dependent. Thus, when a batch showing negligible aggregation (<5%) was used, the reconstructed dimer exhibited T_m and ΔH_{cal} values very close to those of native PSP-I/PSP-II (Figure 4, Table 2). This result corroborates that PSP-I and PSP-II are capable of fully reassociating into a native-like heterodimer.

The presence of Zn^{2+} drastically decreased the thermal stability of PSP-I, the T_m dropping to around 27.7 °C (Table 2). However, the broadening of the heat-capacity curve and the low enthalpy of denaturation, together with the irreversibility of the process, made further analysis of the transition curve unfeasible. In contrast, no significant effect of Zn^{2+} on the thermostability of PSP-II was observed (Table 2).

Circular Dichroism Spectroscopy. The near-UV CD spectrum of PSP-I resembled that of PSP-I/PSP-II (*16*), showing a large negative band with minima at 287 and 268 nm and a sharp positive band at 290 nm in the tryptophan region (Figure 5A). The thermal denaturation of PSP-I led to a gradual decrease in the intensity of positive and negative bands (Figure 5B), along with an increase in ellipticity below 250 nm. These changes were irreversible and reflect the loss of the tertiary structure of the protein. The ellipticity at 268 nm was monitored as a convenient probe of thermal denaturation (Figure 5B, inset). The experimental curves

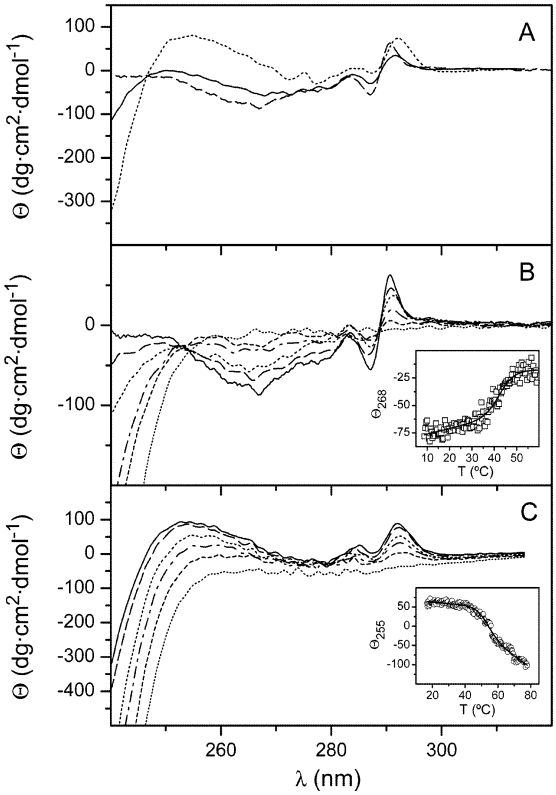

FIGURE 5: Near-UV CD of PSP-I and PSP-II; variation with temperature. (A) Spectra were obtained at 20 °C for 1 mg mL^{-1} of PSP-I (----) and PSP-II (....) solutions in 20 mM Hepes at pH 7.0. The solid line corresponds to the control PSP-I/PSP-II heterodimer. (B) Representative PSP-I spectra acquired at 5 (solid line), 20 (dashed line), 35 (dotted line), 45 (dash−dotted line), 50 (short dashed line), and 70 (short dotted line) °C. (C) Representative PSP-II spectra acquired at 15 (solid line), 30 (dashed line), 50 (dotted line), 55 (dash−dotted line), 60 (short dashed line), and 70 (short dotted line) °C. Insets in B and C show the variation with temperature of ellipticity at 268 and 255 nm, respectively. The continuous lines correspond to the fit of a sigmoidal function to experimental data.

were phenomenologically analyzed using a sigmoidal function (see Experimental Procedures) and yielded a value of 43.6 ± 0.6 °C for $T_{1/2}$. This value is very close to the transition temperature obtained by DSC (Table 2).

The near-UV spectrum of PSP-II also presented a positive band in the tryptophan region but differed significantly at shorter wavelengths from those of PSP-I and the PSP-I/PSP-II heterodimer, showing a broad positive region with a maximum at 255 nm (Figure 5A). The intensity of these bands varied with the degree of PSP-II aggregation and decreased irreversibly upon thermal denaturation with a concomitant increase in ellipticity below 250 nm (Figure 5C). From the monitoring of the decrease with temperature of the ellipticity at 255 nm (Figure 5C, inset), a $T_{1/2}$ value of 52.6 ± 0.6 °C was estimated. This value is also close to the transition temperature obtained by DSC (Table 2).

The far-UV CD spectrum of PSP-I was also very similar to that of the PSP-I/PSP-II heterodimer (*24*), with a large positive band centered around 201 nm and a negative band at 216 nm (Figure 6A). Deconvolution of the spectra using the Lincomb procedure showed that in solution the major structural elements of PSP-I are β-sheets and turns (over 65% of β-structure), which is consistent with the structure observed by X-ray crystallography. A similar far-UV CD

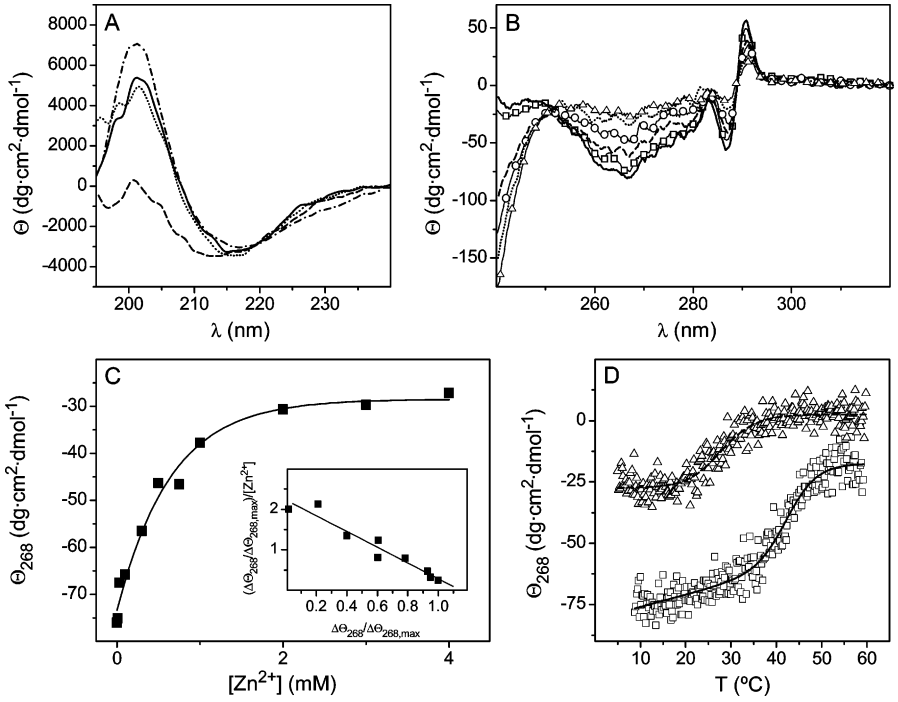

FIGURE 6: Effect of Zn^{2+} on the CD spectra of PSP-I. (A) Far-UV CD spectra were acquired at 5 °C for 1 mg mL^{-1} of PSP-I solutions in 20 mM Hepes at pH 7.0 in the absence (—) or presence of 1 mM Zn^{2+} (----) or 1 mM Ca^{2+} (.....). The dash−dot line (-·-·-) corresponds to the control PSP-I/PSP-II heterodimer. (B) Near-UV CD spectra were acquired, as in Figure 5A, in the absence (—) or presence of 30 μM (-□-), 300 μM (----), 750 μM (-○-), 2 mM (....) or 4 mM (-△-) Zn^{2+}. (C) Variation in ellipticity at 268 nm (Θ_{268}) as a function of Zn^{2+} concentration. Inset: Scatchard plot of the data in terms of relative ellipticity changes ($\Delta\Theta_{268}/\Delta\Theta_{268,max}$), taking $\Delta\Theta_{268,max}$ as the difference in Θ_{268} between 0 and 4 mM Zn^{2+}. (D) Variation with temperature of Θ_{268} in the absence (□) or presence of 4 mM Zn^{2+} (△). The continuous lines correspond to the fit of a sigmoidal function to experimental data.

spectrum was also observed for PSP-II, although the intensity of the bands varied, again, with the degree of aggregation.

The addition of Zn^{2+} to the PSP-I solution (in 20 mM HEPES at pH 7) resulted in a decrease in the secondary-structure content of the protein, whereas Ca^{2+} induced no observable effect (Figure 6A). At 1 mM $ZnCl_2$, a loss of 30% in β-structure was estimated. Furthermore, the near-UV spectrum underwent similar changes, although not identical to those produced by thermal denaturation (Figure 6B) showing a decrease in the intensity of the positive and negative bands and an increase in ellipticity below 250 nm. These changes were dependent on the Zn^{2+} concentration, as clearly evidenced by the Θ_{268} versus [Zn^{2+}] plot (Figure 6C). A Scatchard analysis of these data, taking the relative decrease in ellipticity at a given Zn^{2+} concentration ($\Delta\Theta_{268}/\Delta\Theta_{268,max}$) as the saturation function, yielded a straight line ($R = 0.97$) (Figure 6C, inset) from which an apparent binding constant for Zn^{2+} of 2.0 ± 0.2 mM^{-1} was estimated. Monitoring the decreasing ellipticity at 268 nm with increasing temperature (Figure 6D) confirmed the reduction in the thermal stability of PSP-I in the presence of Zn^{2+} revealed by DSC (Table 2). The ellipticity change associated with the PSP-I thermal denaturation and the slope of the CD profiles were also smaller, indicating that Zn^{2+} perturbed the protein structure and decreased the cooperativity of the denaturalization process, despite the PSP-I self-association induced by the cation.

Although the above-mentioned effects were observed immediately after the addition of $ZnCl_2$ to PSP-I, the incubation of the samples for longer periods (1−24 h) resulted in a further and progressive decrease in the intensity of the bands (Figure 7A). This indicates the existence of a

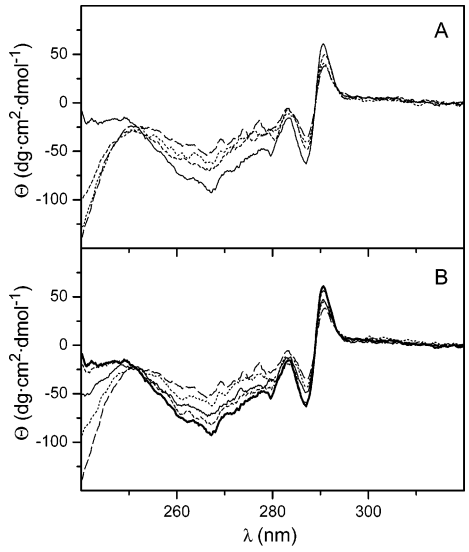

FIGURE 7: Time dependence of the Zn^{2+}-induced changes in the near-UV CD spectrum of PSP-I; reversal by EDTA. (A) Spectra were acquired for 1 mg mL^{-1} of PSP-I solutions in 20 mM Hepes at pH 7.0, in the absence (solid line) or presence of 300 μM Zn^{2+}, either immediately upon the addition of the cation to the protein solution (short dashed line) or after incubation for 5 h (dotted line), or 24 h (dashed line). (B) After incubation for 24 h with 300 μM Zn^{2+} (dashed line), 1 mM EDTA was added and the spectrum acquired after incubation for 20 h (dotted line). Finally, additional EDTA was added up to a final concentration of 10 mM and the spectrum obtained immediately (thin solid line) and after incubation for 3 days (short dashed line). The thick solid line denotes the control PSP-I. All spectra were acquired at 5 °C, and the incubations were performed at the same temperature.

second slow Zn^{2+}-induced process, as revealed by the analytical centrifugation studies. Both events could be almost

completely reversed by adding EDTA. The recovery induced by EDTA was very slow and dependent on its concentration (Figure 7B). Thus, the spectrum changes promoted by the incubation of PSP-I with 0.3 mM Zn^{2+} for 24 h were about 75% reverted after the incubation with 10 mM EDTA for 3 days. In contrast, no effect of Ca^{2+} on the CD spectra of PSP-I was observed. Interestingly, the effect of Zn^{2+} on both the far-UV and near-UV CD spectra became negligible when the pH of the PSP-I solution was lowered to 6; this suggests the possible involvement of histidine residues in Zn^{2+} coordination. No appreciable effect of Zn^{2+} on the CD spectra of PSP-II was discerned.

Affinity Chromatography on Heparin-Acrylic Beads. In a previous study (*8*), no binding of radioiodinated PSP-I to heparin immobilized on plastic microwells was observed. However, low-affinity interactions might not have been detected in this binding assay because of the minute, nanomolar concentrations of protein and ligand present in the well. On the contrary, PSP-I has been found in the fraction of seminal plasma bound to a Sepharose−heparin column (*25*). Therefore, here, we have examined the chromatographic behavior of PSP-I on heparin immobilized on acrylic beads to minimize possible interfering interactions with the support. Negligible binding of PSP-I to the heparin-acrylic bead column equilibrated with TBS containing 2 mM EDTA was observed. In contrast, in the presence of 1 mM Zn^{2+}, most of the protein was retained in the column and could be eluted by the addition of 1 M NaCl (data not shown). Alternatively, the bound protein could also be eluted by the addition of free competing heparin (10 mg/mL) to the buffer. However, chondroitin-6-sulfate, a different sulfated polysaccharide, was ineffective for desorbing bound PSP-I from the column at the same concentration. This behavior suggests a seemingly specific recognition of heparin by PSP-I in the presence of Zn^{2+}.

DISCUSSION

The first salient conclusion that can be drawn from this study is that separate spermadhesins PSP-I and PSP-II seem to preserve the overall fold of the CUB domain observed in the crystal structure of the PSP-I/PSP-II heterodimer. The isolated subunits behave in solution as monomeric proteins, although PSP-II often shows a variable degree of aggregation. Moreover, the hydrodynamic shape and dimensions of the PSP-I monomer, deduced from sedimentation velocity studies, are comparable to those found for the ellipsoidal subunits of the PSP-I/PSP-II heterodimer. In addition, the similarity of the far- and near-UV CD spectra to those of the heterodimer (*24*) supports the conservation of secondary and tertiary structures in the isolated subunits. In particular, the near-UV CD spectra are characterized by the presence of a sharp positive band in the tryptophan absorption region. Both PSP-I and PSP-II contain a single tryptophan residue, which is accommodated within the hydrophobic core of the CUB domain in the PSP-I/PSP-II structure. Thus, the Trp band reflects the specific environment of this residue in the folded tertiary structure, and it can be regarded as a characteristic fingerprint of the native fold of PSP-I and PSP-II. In addition, a preliminary inspection of the ^1H NMR spectrum of PSP-I has revealed the presence of narrow lines and significant shift dispersion, together with a large number of signals in the aromatic region and signal dispersion beyond 8.5 ppm and below 0 ppm (data not shown); this data further supports the conclusion that PSP-I is a folded and well-ordered protein.

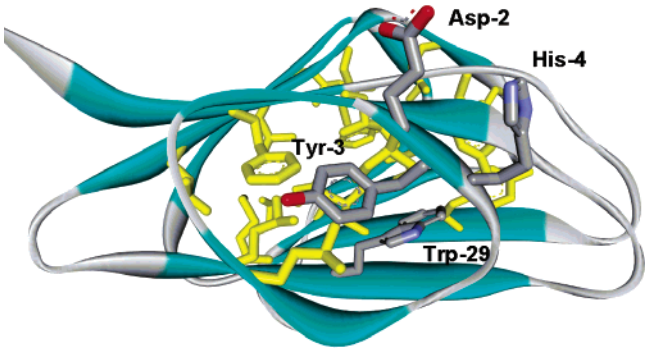

FIGURE 8: Ribbon diagram of PSP-I showing the relative position of residues Asp-2, Tyr-3, and His-4 with respect to the hydrophobic core. Residues of the hydrophobic core are colored in yellow, except for Tyr-3 and Trp-29, which are colored in CPK code. The residues are numbered according to the amino acid sequence of the mature protein.

Bearing in mind that no major changes in the architecture of the subunits seem to occur upon dissociation of the PSP-I/PSP-II heterodimer, the higher thermostability of the dimer over the isolated subunits, detected by DSC and CD thermal denaturation experiments, can be primarily attributed to intersubunit interactions. Besides, the heterodimer interface is largely nonpolar, consisting of a central solvent-inaccessible hydrophobic nucleus flanked on both sides by a cluster of polar or charged residues and a solvent exposed aromatic residue (*14*). The desolvation of this hydrophobic nucleus will definitely contribute to an increase in the denaturation enthalpy change and thermostability of the dimer.

A second major conclusion is that PSP-I stability is notably diminished in the presence of Zn^{2+} as evidenced by DSC and CD, whereas no effect on PSP-II is observed. Changes in the CD spectra of PSP-I are indicative of a loosened protein core packing and a decrease in the content of the secondary structure. The critical dependence on the pH of these changes is compatible with histidine residues being involved in metal ion coordination, as is frequently found in Zn^{2+}−protein complexes. PSP-I contains two histidine residues at positions 4 and 95 of the protein amino acid sequence. Although His-95 is located on a loop far away from the protein core, His-4 is at the end of β-strand 1, which holds Tyr-3 (Figure 8). This tyrosine residue lies on top of the hydrophobic core and acts like a small lid. Thus, it is conceivable that a displacement of this short β-strand as a result of Zn^{2+} coordination by His-4 and also possibly Asp-2 may shift the lid and expose the core residues, thus decreasing the stability of the domain. Moreover, the exposure of a hydrophobic region on the protein surface could account for the self-association of PSP-I, as reported, for example, for calreticulin (*26*), which, in the presence of Zn^{2+}, associates reversibly into dimers and precipitates at high concentrations of the cation. At Zn^{2+} concentrations in the order of the total amounts found in seminal plasma, the predominant PSP-I species is also a dimer. Yet, Zn^{2+} binding is not apparently mediated by two different PSP-I molecules as has been proposed for other proteins such as the Alzheimer's amyloid β-peptide (*27*) because changes in the CD spectra are manifestly perceptible at concentrations below

those inducing the protein self-association. The effects of Zn^{2+} on PSP-I provide a rationale for the previously reported decrease in stability of the PSP-I/PSP-II heterodimer (*16*). Evidently, the dissociation of the heterodimer (detectable at the low nanomolar range of protein concentrations) will be enhanced in the presence of the cation because of the Zn^{2+}-induced unfolding and self-association of PSP-I.

A final noteworthy observation is that the Zn^{2+}-mediated structural changes in PSP-I have a profound effect on its heparin-binding capability. Although in the absence of Zn^{2+} PSP-I is not retained on a heparin-acrylic bead column, in the presence of the cation, the protein is bound and eluted with 1 M NaCl, resembling the behavior of the free PSP-I present in the heparin-binding fraction of seminal plasma. The fact that heparin but not chondroitin-6-sulfate behaves as the effective competitor for the desorption of bound PSP-I suggests that binding to the heparin column does not merely result from a nonspecific ion exchange process. Thus, only Zn^{2+}-denatured and self-associated PSP-I exhibits a seemingly specific heparin-binding capability in the assayed system. The activation of the heparin-binding activity through protein oligomerization is not an unusual strategy, and it has been previously reported for the bovine seminal plasma protein PDC-109 (*28*) and other unrelated biological systems such as the above-mentioned amyloidogenic β-peptide (*29*). Of note is the fact that spermadhesins in the heparin-binding fraction of boar seminal plasma appear as polydisperse proteins exhibiting different aggregation states. We propose that the modulation by Zn^{2+} of the structural organization of PSP-I might be a physiological phenomenon and that an analogous modulation could underlie the behavior of other porcine spermadhesins, with the already known exception of PSP-II, which exhibits heparin-binding activity in the absence of Zn^{2+} (*8*). Nonetheless, PSP-I is predominantly found in seminal plasma with a well-folded structure as a partner of PSP-II in the PSP-I/PSP-II heterodimer, whose integrity is ensured, even in the presence of zinc ions, by the high concentration of both PSP-I and PSP-II spermadhesins. Thus, PSP-I is an unusual example of an intrinsically structured protein showing a dual conformational status with different ligand-binding capabilities within the same physiological environment: a well-folded protein associated to PSP-II in the PSP-I/PSP-II heterodimer and a denatured, self-associated protein exhibiting heparin-binding.

The interaction of spermadhesins with heparin-like glycosaminoglycans present in the female reproductive tract is thought to mediate sperm capacitation (*2*). Although the dilution of semen within the genital tract fluids probably decreases the immediate availability of Zn^{2+}, the slow reversion of the Zn^{2+}-induced changes evidenced by CD spectroscopy may guarantee the preservation of the heparin-binding capability while required. In this context, it is important to emphasize that boar spermadhesins are predominantly synthesized in the seminal vesicle, where Zn^{2+} concentration is even higher than in seminal plasma (up to 2 mM (*17*)). Thus, a Zn^{2+}-induced conformational state may occur even before the mixture, at ejaculation, of secretions from seminal vesicles, prostate and bulbourethral glands, and the testicular/epididymal fluid. Non-PSP-II-complexed PSP-I, together with spermadhesins AQN-1, AQN-3, AWN-1, and AWN-2 have been found to become coated on ejaculated spermatozoa, the bulk of this spermadhesin coat being released during subsequent in vitro sperm capacitation (*7*). However, the involvement of the spermadhesin PSP-I/PSP-II complex in capacitation-related events has not been demonstrated, probably because heterodimerization modulates the biological activities of the subunits. Accumulating evidence points to a role for these spermadhesins as exogenous modulators of uterine immune activity. Hence, PSP-I and PSP-II are immunostimulatory for lymphocyte activity in vitro (*30*), and the binding of PSP-I to lymphocytes has been demonstrated (*31*). Furthermore, the PSP-I/PSP-II heterodimer and its isolated subunits induce the recruitment of neutrophils into the peritoneal cavity of rats (*32*) and pigs (*33*). In the rat, the neutrophil migration-inducing activity of PSP-I/PSP-II, and possibly of the PSP-II subunit, is mediated by the stimulation of resident macrophages, which release a neutrophil chemotactic substance (*32*), whereas PSP-I appears to act directly on neutrophils (*34*). Thus, the dissociation of the heterodimer upon the dilution of the protein in the female genital tract might be of physiological importance for the immune modulation inside the uterus. The purpose of these proinflammatory and immunostimulatory activities would be to prevent possible infections of the lower reproductive tract and to purge the uterine environment of foreign cells for the descending early embryos, thus ensuring reproductive success.

ACKNOWLEDGMENT

We thank V. López Moyano for technical assistance and Dr. Miguel Angel Treviño for the pilot NMR studies.

REFERENCES

1. Töpfer-Petersen, E., Calvete, J. J., Sanz, L., and Sinowatz, F. (1995) Carbohydrate- and heparin-binding proteins in mammalian fertilization, *Andrologia 27*, 303−324.
2. Calvete, J. J., Sanz, L., Dostàlovà, Z., and Töpfer-Petersen, E. (1995) Spermadhesins: sperm-coating proteins involved in capacitation and zona pellucida binding, *Fertilität 11*, 35−40.
3. Bergeron, A., Villemure, M., Lazure, C., and Manjunath, P. (2005) Isolation and characterization of the major proteins of ram seminal plasma, *Mol. Reprod. Dev. 71*, 461−470.
4. Töpfer-Petersen, E., Romero, A., Varela, P. F., Ekhlasi-Hundrieser, M., Dostàlovà, Z., Sanz, L., and Calvete, J. J. (1998) Spermadhesins: a new protein family. Facts, hypotheses and perspectives, *Andrologia 30*, 217−224.
5. Jansen, S., Ekhlasi-Hundrieser, M., and Topfer-Petersen, E. (2001) Sperm adhesion molecules: structure and function, *Cells Tissues Organs 168*, 82−92.
6. Haase, B., Schlotterer, C., Ekhlasi-Hundrieser, M., Kuiper, H., Distl, O., Topfer-Petersen, E., and Leeb, T. (2005) Evolution of the spermadhesin gene family, *Gene 352*, 20−29.
7. Dostàlovà, Z., Calvete, J. J., Sanz, L., and Töpfer-Petersen, E. (1994) Quantitation of boar spermadhesins in accessory sex gland fluids and on the surface of epididymal, ejaculated and capacitated spermatozoa, *Biochim. Biophys. Acta 1200*, 48−54.
8. Solís, D., Romero, A., Jiménez, M., Díaz-Mauriño, T., and Calvete, J. J. (1998) Binding of mannose-6-phosphate and heparin by boar seminal plasma PSP-II, a member of the spermadhesin protein family, *FEBS Lett. 431*, 273−278.
9. Calvete, J. J., Mann, K., Schäfer, W., Raida, M., Sanz, L., and Töpfer-Petersen, E. (1995) Boar spermadhesin PSP-II: location of posttranslational modifications, heterodimer formation with PSP-I glycoforms and effect of dimerization on the ligand-binding capabilities of the subunits, *FEBS Lett. 365*, 179−182.
10. Kwok, S. C. M., Soares, M. J., McMurtry, J. P., and Yurewicz, E. C. (1993) Binding characteristics and immunolocalization of porcine seminal protein, PSP-I, *Mol. Reprod. Dev. 35*, 244−250.
11. Jonáková, V., Maňásková, P., Graus, M., Liberda, J., and Tichá, M. (2000) Sperm surface proteins in mammalian fertilization, *Mol. Reprod. Dev. 56*, 275−277.

12. Dostàlovà, Z., Calvete, J. J., and Töpfer-Petersen, E. (1995) Interaction of nonaggregated boar AWN-1 and AQN-3 with phospholipid matrices. A model for coating of spermadhesins on the sperm surface, *Biol. Chem. Hoppe-Seyler 376*, 237−242.
13. Maňásková, P., Liberda, J., Tichá, M., and Jonáková, V. (2000) Aggregated and monomeric forms of proteins in boar seminal plasma: characterization and binding properties, *Folia Biol. (Prague) 46*, 143−151.
14. Varela, P. F., Romero, A., Sanz, L., Romão, M. J., Töpfer-Petersen, E., and Calvete, J. J. (1997) The 2.4 Å resolution crystal structure of boar seminal plasma PSP-I/PSP-II: a zona pellucida-binding glycoprotein heterodimer of the spermadhesin family built by a CUB domain architecture, *J. Mol. Biol. 274*, 635−649.
15. Bork, P., and Beckmann, G. (1993) The CUB domain. A widespread module in developmentally regulated proteins, *J. Mol. Biol*. *231*, 539−545.
16. Campanero-Rhodes, M. A., Menéndez, M., Sáiz, J. L., Sanz, L., Calvete, J. J., and Solís, D. (2005) Analysis of the stability of the spermadhesin PSP-I/PSP-II heterodimer. Effects of Zn^{2+} and acidic pH, *FEBS J. 272*, 5663−5670.
17. Boursnell, J. C., Baronos, S., Briggs, P. A., and Butler, E. J. (1972) The concentrations of zinc in boar seminal plasma and vesicular secretion in relation to those of nitrogenous substances, citrate, galactose and fructose, *J. Reprod. Fert. 29*, 215−227.
18. Arver, S., and Eliasson, R. (1980) Zinc and magnesium in bull and boar spermatozoa, *J. Reprod. Fertil. 60*, 481−484.
19. Minton, A. P. (1994) Conservation of signal: a new algorithm for the elimination of the reference concentration as an independently variable parameter in the analysis of sedimentation equilibrium, in *Modern Analytical Ultracentrifugation* (Schuster, T. H., and Laue, T. H., Eds), pp 81−93, Birkhäuser, Boston, MA.
20. Schuck, P. (2000). Size distribution analysis of macromolecules by sedimentation velocity ultracentrifugation and lamm equation modelling, *Biophys. J. 78*, 1606−1619.
21. Nimtz, M., Grabenhorst, E., Conradt, H. S., Sanz, L., and Calvete, J. J. (1999) Structural characterization of the oligosaccharide chains of native and crystallized boar seminal plasma spermadhesin PSP-I and PSP-II glycoforms, *Eur. J. Biochem. 265*, 703−718.
22. Laue, T. M., Shah, B. D., Ridgeway, T. M., and Pelletier, S. L. (1992) Computer-aided interpretation of analytical sedimentation data for proteins, in *Analytical Ultracentrifugation in Biochemistry and Polymer Science* (Harding, S. E., Rowe, A. J., and Horton, J. C., Eds), pp 90−125, Royal Society of Chemistry, Cambridge, U.K..
23. Perczel, A., Park, K., and Fasman, G. D. (1992) Deconvolution of the circular dichroism spectra of proteins: The circular dichroism spectra of antiparallel β-sheet in proteins, *Proteins 13*, 57−69.
24. Menéndez, M., Gasset, M., Laynez, J., López-Zumel, C., Usobiaga, P., Töpfer-Petersen, E., and Calvete, J. J. (1995) Analysis of the structural organization and thermal stability of two spermadhesins. Calorimetric, circular dichroic and Fourier transform infrared spectroscopic studies, *Eur. J. Biochem. 234*, 887−896.
25. Calvete, J. J., Solís, D., Sanz, L., Díaz-Mauriño, T., Schäfer, W., Mann, K., and Töpfer-Petersen, E. (1993) Characterization of two glycosylated boar spermadhesins, *Eur. J. Biochem. 218*, 719−725.
26. Li, Z., Stafford, W. F., and Bouvier, M. (2001) The metal ion binding properties of calreticulin modulate its conformational flexibility and thermal stability, *Biochemistry 40*, 11193−11201.
27. Miura, T., Suzuki, K., Kohata, N., and Takeuchi, H. (2000) Metal binding modes of Alzheimer's amyloid β-peptide in insoluble aggregates and soluble complexes, *Biochemistry 39*, 7024−7031.
28. Calvete, J. J., Campanero-Rhodes, M. A., Raida, M., and Sanz, L. (1999) Characterization of the conformational and quaternary structure-dependent heparin-binding region of bovine seminal plasma protein PDC-109, *FEBS Lett. 444*, 260−264.
29. Watson, D. J., Lander, A. D., and Selkoe, D. J. (1997) Heparin-binding properties of the amyloidogenic peptides Aβ and amylin, *J. Biol. Chem. 272*, 31617−31624.
30. Leshin, L. S., Raj, S. M., Smith, C. K., Kwok, S. C., Kraeling, R. R., and Li, W. I. (1998) Immunostimulatory effects of pig seminal proteins on pig lymphocytes, *J. Reprod. Fertil. 114*, 77−84.
31. Yang, W. C., Kwok, S. C. M., Leshin, S., Bollo, E., and Li, W. I. (1998) Purified porcine seminal plasma protein enhances in vitro immune activities of porcine peripheral lymphocytes, *Biol. Reprod. 59*, 202−207.
32. Assreuy, A. M., Calvete, J. J., Alencar, N. M. N., Cavada, B. S., Rocha-Filho, D., Melo, S., Cunha, F., and Ribeiro, R. (2002) Spermadhesin PSP-I/PSP-II heterodimer and its isolated subunits induced neutrophil migration into the peritoneal cavity of rats, *Biol. Reprod. 67*, 1796−1803.
33. Rodriguez-Martinez, H., Saravia, F., Wallgren, M., Tienthai, P., Johannisson, A., Vázquez, J. M., Martínez, E., Roca, J., Sanz, L., and Calvete, J. J. (2005) Boar spermatozoa in the oviduct, *Theriogenology 63*, 514−535.
34. Assreuy, A. M. S., Alencar, N. M. N., Cavadam B. S., Rocha-Filho, D. R., Feitosa, R. F. G., Cunha, F. Q., Calvete, J. J., and Ribeiro, R. A. (2003) Porcine spermadhesin PSP-I/PSP-II stimulates macrophages to release a neutrophil chemotactic substance: modulation by mast cells, *Biol. Reprod. 68*, 1836−1841.

BI052621G